②

AD-A223 175

te technical note techni

MLS Mathematical Model Validation Study Using Airborne MLS Data from Midway Airport Engineering Flight Tests, August 1988

Linda Pasquale
Jesse D. Jones

DTIC
ELECTE
JUN 21 1990
S D
D

April 1990

DOT/FAA/CT-TN90/2

DISTRIBUTION STATEMENT A
Approved for public release;
Distribution Unlimited

U.S. Department of Transportation
Federal Aviation Administration

Technical Center
Atlantic City International Airport, N.J. 08405

90 06 21 095

1. Report No.	2. Government Accession No.	3. Recipient's Catalog No.
DOT/FAA/CT-TN90/2		

4. Title and Subtitle	5. Report Date
MLS MATHEMATICAL MODEL VALIDATION STUDY USING AIRBORNE MLS DATA FROM MIDWAY AIRPORT ENGINEERING FLIGHT TESTS, AUGUST 1988	April 1990
	6. Performing Organization Code
	ACD-330

7. Author's)	8. Performing Organization Report No.
Linda Pasquale and Jesse D. Jones	DOT/FAA/CT-TN90/2

9. Performing Organization Name and Address	10. Work Unit No. (TRAIS)
Department of Transportation Federal Aviation Administration Technical Center Atlantic City International Airport, N.J. 08405	
	11. Contract or Grant No.
	T06-038
	13. Type of Report and Period Covered

12. Sponsoring Agency Name and Address	
Department of Transportation Federal Aviation Administration Maintenance and Development Service Washington, D.C. 25090	Technical Note March 1989
	14. Sponsoring Agency Code

15. Supplementary Notes

16. Abstract

This Microwave Landing System (MLS) mathematical model validation study evaluated the performance of the MLS math model by comparing the results of the model's simulation of flight test profiles flown at Midway Airport in Chicago with actual airborne data collected during the test flights. The study specifically addressed the problems of scattering and shadowing of MLS signals by buildings in the airport environment.

The study found that comparisons of model output with real world data showed good agreement. Discrepancies between the two were explainable as either the model's sensitivity to input parameters or the model's "worst case scenario" strategy. The study supports the conclusion that the MLS math model is a valuable tool for use in the evaluation of potential sources of signal interference for an MLS system configuration in a particular airport environment.

17. Key Words	18. Distribution Statement
Midway Airport MLS Microwave Landing System Mathematical Modeling	This document is available to the U.S. public through the National Technical Information Service, Springfield, Virginia 22161.

19. Security Classif. (of this report)	20. Security Classif. (of this page)	21. No. of Pages	22. Price
Unclassified	Unclassified	42	

Form DOT F 1700.7 (8-72)   Reproduction of completed page authorized

TABLE OF CONTENTS

Page

iii

LIST OF ILLUSTRATIONS

LIST OF ILLUSTRATIONS (CONTINUED)

EXECUTIVE SUMMARY

This Microwave Landing System (MLS) mathematical model validation study evaluated the performance of the MLS math model by comparing the results of the model's simulation of flight test profiles flown at Midway Airport in Chicago with actual airborne data collected during the test flights. The study specifically addressed the problems of scattering and shadowing of MLS signals by buildings in the airport environment.

The study found that comparisons of model output with real world data showed good agreement. Discrepancies between the two were explainable as either the model's sensitivity to input parameters or the model's "worst case scenario" strategy. The study supports the conclusion that the MLS math model is a valuable tool for use in the evaluation of potential sources of signal interference for an MLS system configuration in a particular airport environment.

INTRODUCTION

PURPOSE.

The purpose of this validation study is to evaluate the performance of the Microwave Landing System (MLS) Mathematical Model by comparing the results of the math model's simulation of flight test profiles flown at Midway Airport in Chicago with actual airborne data collected during the test flights. Specifically, this study addresses the problems of scattering and shadowing of MLS signals by buildings in the airport environment. The approach to validation taken in this study and the philosophy of interpreting the results are discussed in detail in Concepts Analysis Division Report ACD-330-90-04, "Approach to Validation of the MLS Mathematical Model," Linda Pasquale and Jesse D. Jones, January 1990.

BACKGROUND.

THE MLS MATHEMATICAL MODEL.
The MLS Mathematical Model simulates the operation of an MLS for the purpose of predicting the effects of the airport environment on the transmitted signal and the corresponding accuracy and usefulness of the signal arriving at the receiver for providing positional information. Three categories of input data define the scenario to be modeled. One set of data describes the airport environment with emphasis on the obstacles (buildings, aircraft, terrain features) that might have reflective (multipath) or diffractive (shadowing) effects on the transmitted signal. Another set of data defines the position and signal characteristics of the MLS antenna systems, and a third set provides the coordinates of the flightpath. The model uses these data to predict (1) the characteristics of the propagated signal and (2) the receiver output angle errors caused by the scenario configuration.

Originally developed by the Lincoln Laboratory of the Massachusetts Institute of Technology, the math model has been extensively revised and baselined by personnel at the Federal Aviation Administration (FAA) Technical Center. Additional testing of the model is required to determine whether the model continues to perform satisfactorily in representing the real world and to investigate the model sensitivities to input parameters.

MLS DEMONSTRATION AT MIDWAY AIRPORT.
At the request of the Great Lakes Region, the FAA Technical Center conducted an operational demonstration of the MLS temporarily installed to serve runway 22L at Chicago's Midway Airport during August 1988. Preparation for the demonstration included three engineering flight tests, conducted on August 27, 28, and 29, 1988, to verify and characterize system performance and to ensure the operational feasibility of the proposed demonstration flight profiles. MLS data recorded during these flight tests provide "real world" data which can be compared with math model predictions, thereby providing an opportunity to evaluate the performance of the model in simulating the Midway Airport environment. This environment includes several tall structures (buildings, aircraft hangars, etc.), both within the airport perimeter and in the downtown Chicago area, which can have scattering or shadowing effects on the MLS signal. Use of a Radio Telemetering Theodolite (RTT) during approaches allows independent (non-MLS) confirmation of some of the angle data.

1

DATA COLLECTION AND REDUCTION METHODOLOGY

MLS EQUIPMENT AND SITING.

Azimuth and elevation stations from the MLS test bed system at the FAA Technical Center were transported via truck to Chicago for the Midway Airport demonstration. The MLS test bed is a modified Bendix FAR-171 MLS (models B-21.5-40S and BI-60S) which meets the FAA MLS accuracy tolerances FAA-STD-022b and FAA-STD-022c. The azimuth antenna used for the demonstration has a 2° beamwidth with ±40° proportional azimuth guidance, and the elevation antenna has a 1.5° beamwidth with proportional coverage from +0.9° to +15°. The field distance measuring equipment (DME) at Midway was used for ranging because no precision distance measuring equipment (DME/P) was available for these flight tests and demonstrations. For approaches, an RTT provided ground-based tracking angle data for one of the MLS transmitters (azimuth or elevation). Only single axis tracking was performed. A map of the Midway Airport siting and obstacle geometry is shown in figure 1.

ENGINEERING FLIGHT TESTS.

The FAA aircraft used for the flight tests, a Convair-580 (N-91), included a data collection system designed, built, installed, and tested at the Technical Center prior to departure. This system records data from the MLS angle receivers, the DME interrogator, and the RTT, when used. Flight profiles (figure 2) include untracked, level partial orbits through the MLS coverage volume for 1.6° and 3.6° elevation angles at distances of 7 and 11 nautical miles (nmi) from the DME. The current RTT cannot be used for tracking during partial orbits because of angular range limitations. Partial orbits, at distances beyond obstacles in the airport environment, allow evaluation of effects on the MLS signal from buildings both on the airport (7 nmi radius) and in the downtown Chicago area (11 nmi radius) for flightpaths both in direct line of sight of the MLS antenna (3.6°) and below the top of the tall buildings (1.6°). Tracked approaches from a range of approximately 10 nmi from threshold at angles of 3.0°, 3.4°, and 3.6° demonstrate MLS capabilities for standard approach flightpaths. A list of the profiles flown (with tracking indicated) that were analyzed for this validation study is shown in table 1.

FLIGHTPATH CREATION.

Flightpath data can be entered into the MLS math model in one of two ways. The coordinates of the flightpath segment endpoints can be included in the formatted input file, a method appropriate for theoretical flightpaths that are calculated mathematically. In the alternate method, the model reads flightpath coordinates directly from a second input file. This method allows the flightpath to be defined in greater detail and is the appropriate method to use when actual flight data are available. The second method, using the measured flightpath input file, was used for this validation study.

Flightpaths are created from the data collected during the engineering flight tests using the RTT angle data in place of the corresponding MLS azimuth or elevation angle data wherever possible. The angle and distance data are translated into X,Y,Z flightpath coordinates by an algorithm known as "Case 12." The Case 12 algorithm is documented in Technical Note DOT/FAA/CT-TN87/2,

2

TABLE 1. MIDWAY ENGINEERING FLIGHT TEST PROFILES AND TRACKING.

Date	Run Seq #	Run Type and Number	Start Time	EL Angle (deg)	AZ Angle	Range	m.s.l. (ft)		RTT for
8/27	1	CCW Orbit 1	05:56:50	3.6	+/-40 deg	11 DME	4900		None
	4	CW Orbit 4	06:26:23	1.6	-/+40 deg	11 DME	2400		None
	6	CW Orbit 6	06:39:44	3.6	-/+40 deg	7 DME	3000		None
	7	Approach 1	06:53:17	3.6	Centerline	From 10 DME	3100	Intercept	AZ
	8	Approach 2	07:15:10	3.6	Centerline	From 10 DME	3100	Intercept	AZ
	9	Approach 3	07:35:45	3.4	Centerline	From 10 DME	3100	Intercept	AZ
	10	Approach 4	07:45:54	3.4	Centerline	From 10 DME	3100	Intercept	AZ
	11	Approach 5	07:56:51	3.0	Centerline	From 10 DME	3100	Intercept	AZ
8/28	1	CCW Orbit 1	09:16:49	1.6	+/-40 deg	7 DME	1700		None
8/29	1	Approach 1	06:32:47	3.6	Centerline	From 10 DME	3100	Intercept	EL
	2	Approach 2	06:44:10	3.6	Centerline	From 10 DME	3100	Intercept	EL
	3	Approach 3	06:55:24	3.4	Centerline	From 10 DME	3100	Intercept	EL
	4	Approach 4	07:06:47	3.4	Centerline	From 10 DME	3100	Intercept	EL
	5	Approach 5	08:07:32	3.0	Centerline	From 10 DME	3100	Intercept	EL
	6	Approach 6	08:18:22	3.0	Centerline	From 10 DME	3100	Intercept	EL

"Helicopter Microwave Landing System Area Navigation (MLS RNAV)," Barry R. Billmann, James H. Remer, and Min-Ju Chang, November 1986. The software developed to reduce and analyze airborne data and create a measured flightpath is documented in Concepts Analysis Division Report ACD-330-90-02, "Data Reduction and Graphics Software for Analysis of Airborne MLS Data," Linda Pasquale, October 1988. In the absence of a completely independent (non-MLS) tracking system, this method produces flightpaths that are the next best approximation to those actually flown by the aircraft.

METHODS OF PLOT GENERATION.

The MLS math model utilizes two stages of simulation. In the first stage, the program BMLST (and the associated plotting program BPLOTT) simulates the signal in space in the specified airport environment and produces plots which identify the multipath and shadowing effects from specific obstacles (buildings, aircraft, ground reflection surfaces). The system model programs BMLSR and BPLOTR in the second stage simulate the operation of the receiver given the transmitted signal as output from BMLST. Plots from this processing stage show the receiver error ("raw" error) which is defined as the difference between the position of the aircraft as it is in "reality" (as defined by the input flightpath) and the position as determined by simulation of the MLS system. These raw error data are further processed with a path following error (PFE) low-pass filter algorithm and a control motion noise (CMN) high-pass filter algorithm. The PFE algorithm, a low-pass filter which removes components of the error data that will not have a measurable effect on the ability of the aircraft to follow the specified flightpath, creates plots that are particularly useful for comparison with actual airborne data because they emphasize the large-scale shape of the data curve. Thus, model output for purposes of this validation study is judged primarily on the basis of the PFE error plots with support from multipath plots which identify specific sources of signal disruption.

The real world data, recorded by the airborne data collection system, are processed by data reduction and graphics software that produce plots designed to facilitate comparison with the model PFE error plots previously described. The specific nature of these plots depends on the type of flightpath and the presence or absence of RTT tracking. Approach flightpaths are described by "differential error" plots which show the angle error against the distance from the azimuth antenna at which the angle is measured. The angle error is calculated by subtracting the RTT angle from the MLS receiver angle (azimuth or elevation) and filtering the resulting value with a PFE algorithm. Similarly, the model receiver error is calculated by subtracting the angle determined from the flightpath coordinates from the angle calculated by the MLS system simulation. The resulting error is PFE filtered. Thus, the model error values and the airborne error values are both PFE filtered and plotted against distance from the MLS azimuth antenna for easy comparison and analysis.

Orbit flightpaths are treated differently because RTT tracking cannot be used for orbits and, therefore, no "error" values can be calculated for airborne data. Consequently, model azimuth and elevation PFE error plots for orbit flightpaths are compared only to plots of the corresponding airborne (MLS receiver output) angle data (PFE filtered). Both values are plotted against the azimuth angle from the MLS azimuth antenna. This allows the plots to be compared with respect to the location and magnitude of multipath and shadowing effects.

4

DATA PRESENTATION AND ANALYSIS

ORBIT FLIGHTPATHS.

In the absence of RTT tracking, model performance for orbit flightpaths must be evaluated by comparing model error plots with plots of recorded airborne data. This is most easily done by considering the azimuth and elevation data separately.

In general, recorded airborne MLS azimuth data indicate no significant effects from obstacles in the airport environment. Figure 3 shows the MLS receiver #1 azimuth angle data plotted against the elapsed time of the flight for run 6 on August 27, a clockwise orbit at 3.6° elevation angle, 7 nmi from DME. This plot is representative of the airborne azimuth data recorded during orbit flightpaths. Even when the flightpath, a clockwise orbit at a 1.6° elevation angle 11 nmi from DME, passes behind and below the tops of the large buildings in downtown Chicago, no effects of the buildings are seen (figure 4).

The results of modeling orbit flightpaths agree with the real world data in predicting no significant interference with the azimuth signal (i.e., no interference causing out-of-tolerance errors). The model does predict some effects from two obstacles that are not evident in the airborne data plots, though in neither case is the resulting error out of tolerance. Figure 5, the dynamic error plot for run 1 on August 27, a 3.6° orbit at 11 nmi from DME, shows a small error at approximately 10° azimuth angle. The error is attributed to shadowing by building 9, the Air Traffic Control Tower's north face. The effect is essentially eliminated after PFE filtering (figure 6). Similarly, figure 7, the dynamic error plot for a 1.6° orbit at 11 nmi from DME (run 4 on August 27) shows errors at approximately 0° azimuth angle attributed to shadowing by the Sears Tower (modeled as building 23). Here, too, the PFE plot (figure 8) shows that the predicted errors are well within tolerance limits. Although the model predicts that the errors caused by these buildings are not significant, an explanation is required as to why any effects appear when none are evident in the airborne data.

Further study of this problem reveals that the model is showing sensitivity to its input parameters. That is, how an obstacle is defined in the input file determines the magnitude of the predicted effect. An example is provided by the Sears Tower for which actual dimensions were unavailable. As mentioned above, figures 7 and 8 show the effect of shadowing by the Sears Tower on the azimuth signal at approximately 0° azimuth angle. For this simulation, the Sears Tower was represented by a plate as defined in figure 9A which approximates the shape of the shadowing silhouette at its base for a "first-try worst-case" scenario. To test the model's sensitivity to input parameters, the simulation was repeated with the Sears Tower defined as in figure 9B, a more refined approximation of the shape of that part of the building that actually shadowed the azimuth signal for a 1.6° orbit. The errors from this shadowing building, shown in figure 10, are reduced, but the effect is still greater than that seen in the airborne data because of the idealized nature of the input. That is, a shadowing building, no matter how it is defined, is "seen" by the model as a single flat rectangular surface with diffraction from all four edges. A real building consists of surfaces that are n r completely flat or smooth and which have no diffraction from the bottom edge. Therefore, the model will usually exaggerate the shadowing

5

effect of any given obstacle. As shown above, this exaggeration can be minimized by representing the shadowing silhouette as a plate (or set of plates) that most closely approximates the shadowing part of the silhouette of the obstacle.

The shadowing effect of the National Guard Hangar presents a special problem for this validation study. Preliminary modeling using a calculated flightpath to simulate a 1.6° orbit at 11 nmi DME predicted a significant shadowing effect from the National Guard Hangar on the azimuth signal. When this flightpath profile was flown at Midway Airport (run 4 on August 27), the MLS receiver lost azimuth signal at approximately 35° azimuth angle (the location of the National Guard Hangar) as indicated by the receiver system flag. This effect cannot be validated by modeling a measured flightpath because the creation of a measured flightpath, in the absence of an independent tracking system, requires MLS azimuth angle data which was not available. However, the location of the loss of MLS guidance corresponds to the region of significant shadowing effect predicted by the model.

The picture presented by the MLS elevation data is also complicated. For orbits at 1.6° elevation and 11 nmi DME (such as run 4 on August 27), the model error plot (figure 11) shows close agreement with MLS receiver elevation angle data (figure 12) in the angular location of strong signal interference between -10° and 0° azimuth angle. The difference in the magnitude of the effect results from the fact that, as with all orbit flightpaths in this validation study, the plots show different types of data. The airborne data plot shows MLS receiver elevation angle data while the model plot shows MLS receiver elevation angle error. The most probable source of the interference is the Esmark Hangar (modeled as building 4). This conclusion is based on the modeling results for orbits at 7 nmi DME. The plots (not included) show a shadowing effect in the same angular location (-10° to 0° azimuth angle) for flightpaths inside the radius of the large downtown buildings, supporting the conclusion that the effect is the result of an obstacle on the airport grounds. The Esmark Hangar is in the location most likely to cause the observed effect. The close agreement of the angular location of the interference effect shown in figures 11 and 12 indicates that the model is correctly simulating the shadowing effects on the elevation system for an orbit flightpath in this scenario.

Signal interference, attributed to the Esmark Hangar, is seen in the same location (-10° to 0°) on the model's PFE error plot for a 3.6° orbit flightpath (11 nmi DME), run 1 on August 27, presented in figure 13. The airborne data (figure 14) does not show this effect clearly, although there is some flattening of the curve between the same azimuth angles (-10° to 0°), also attributed to Esmark Hangar effects. Since the scale for this plot is too coarse to show the effects of the hangar, the plot was expanded in the area of interest (using a finer scale for the Y axis) as shown in figure 15. Figure 15 clearly shows disruption of the trend of the curve in the same azimuth angle region. It is also probable that the model is exaggerating the scattering effects of the Esmark Hangar for this flightpath. This will be discussed in the following section.

APPROACH FLIGHTPATHS.

The model shows good agreement with the airborne data for approach flightpaths. Availability of RTT tracking for approaches allows the creation of differential error plots (from airborne angle data) which are PFE filtered for comparability

with the corresponding model error plots. The results of these comparisons are discussed below for each antenna system.

Figures 16 and 17 show representative examples of the close agreement between model output and airborne data with respect to signal interference on the azimuth signal from the airport environment for approach flightpaths (in this case, a 3.6° approach, run 7 on August 27). Both sets of data show that the azimuth signal is clear of significant interference in this environment. They also illustrate the noisiness of flight data in comparison with modeled data and support the strategy of comparing real world data with model output for large-scale features only.

The elevation system shows more sensitivity to environmental influences for approach flightpaths, as evidenced by the noisiness of the data compared with that of the azimuth system. Both airborne data and model output show this, as illustrated by comparing figures 18 and 19 (run 3 on August 29) with figures 16 and 17. For approaches in general, the airborne data and model output show similar large-scale features but differences in details (compare figures 18 and 19). This disagreement between real world data and model output can be caused by various factors. One possibility is that the RTT optical center was not measured precisely relative to the MLS elevation antenna phase center, thereby introducing a parallax error. Also, an unusually heavy rain soaked the ground (fill) at the elevation site before the flight test of August 29 resulting in a muddy base for the RTT. This may also have caused an inaccurate RTT 0° reference. Another possibility is that the model exaggerates the scattering effects of certain obstacles. The clearest evidence of the model's tendency to exaggerate scattering effects is provided by run 6 on August 29, a 3.0° approach flightpath. The differential error plot (figure 20) though noisy, shows no single major effect. However, the corresponding model error plot (figure 21) clearly presents a significant (though not out-of-tolerance) disturbance between 3 and 4 nmi from the azimuth antenna. Since this effect is seen in almost all of the model output data for approach flightpaths and is the major discrepancy between model output and airborne data for approach flightpaths, further analysis was performed.

The multipath plot for the elevation antenna for run 6 (figure 22) identifies the source of multipath effects as building 4, the Esmark Hangar. One explanation for the model's overestimation of the effect of this building is the model's "worst case scenario" strategy. That is, regardless of the building's surface material specified in the input file, all obstacles are given the default roughness factor of 0 which describes a completely smooth reflecting surface. To test the effect of the roughness factor, the scenario was rerun several times, increasing the default roughness factor on each run. The roughness value is hard-coded in the model software and, therefore, can only be changed by altering model code. This method would not be used for an airport modeling study, but is the only method available for performing these experiments. With a roughness factor of 0.2, the effect of building 4 in both the multipath (figure 23) and error (figure 24) plots is noticeably reduced. With a roughness factor of 0.5, the effect disappears completely (figures 25 and 26). It seems reasonable to conclude, therefore, that the discrepancy between the model output and the airborne data can be explained by the model's "worst case" strategy of assuming that all surfaces are perfectly smooth reflectors. The assignment of a roughness factor more appropriate to each surface material should bring model output into closer agreement with real world conditions.

7

CONCLUSIONS

Comparisons of model output with real world data collected during flight tests at Midway Airport in Chicago generally show good agreement. Discrepancies between measured data and model results are explained either by the model's sensitivity to input parameters or by the model's "worst case scenario" strategy. Thus, at Midway Airport, the model tends to exaggerate the shadowing effects on the azimuth signal of the Sears Tower for orbit flightpaths and the scattering effects of the Esmark Hangar on the elevation signal for approach flightpaths. In the case of shadowing, this exaggeration is a result of the way shadowing obstacles are defined in the input file. More detailed surface definitions for shadowing obstacles will improve model performance in this area. For scattering, the exaggeration is explained by the model's assumption of a perfectly smooth reflecting surface and would be modified by more realistic simulation of the characteristics of reflecting surfaces. In neither case will the results of modeling be misleading if interpreted from the path following error (PFE) filtered error plots showing tolerance limits.

We can conclude, therefore, that the MLS mathematical model adequately simulates the behavior of an Microwave Landing System (MLS) system at Midway Airport in Chicago with respect to the effects of scattering and shadowing buildings on the signals arriving at the receiver. Furthermore, the conclusions drawn from modeling the Midway Airport scenario with measured flightpaths agree with those based on the modeling of Midway with theoretically calculated flightpaths (published in Technical Note DOT/FAA/CT-TN87/49, "Microwave Landing System Mathematical Modeling Study for Midway Airport Runway 22L, Chicago, Illinois," Jesse D. Jones and Linda Epstein, January 1988). That is, neither study found anything in the Midway Airport environment that would cause out-of-tolerance errors. The results of this validation study support the conclusion that the MLS mathematical model is a valuable tool for use in the evaluation of the potential sources of signal interference for an MLS system configuration in a particular airport environment.

RECOMMENDATIONS

It is recommended that:

1. Future validation studies be conducted using a measured flightpath obtained from an independent (non-Microwave Landing System (MLS)) dual-axis tracking system. This would allow the MLS math model to predict MLS errors based on an actual flightpath rather than a flightpath derived from MLS data with inherent errors and would facilitate comparison with real world error data.

2. Measurements be made of the effect of the roughness of various surface materials on the scattering of MLS signals and that the code of the model be modified accordingly.

JOHN
HANCOCK
BLDG. []

SEARS
TOWER []

STANDARD
OIL BLDG. []

(NOT DRAWN TO SCALE)

MIDWAY AIRLINES HANGAR

ESMARK HANGAR

AIR TRAFFIC
CONTROL TOWER ◇

EL △

DME △

NATIONAL GUARD
HANGAR ◇

AZ △

FIGURE 1.   MIDWAY AIRPORT RUNWAY 22L SCENARIO MAP

9
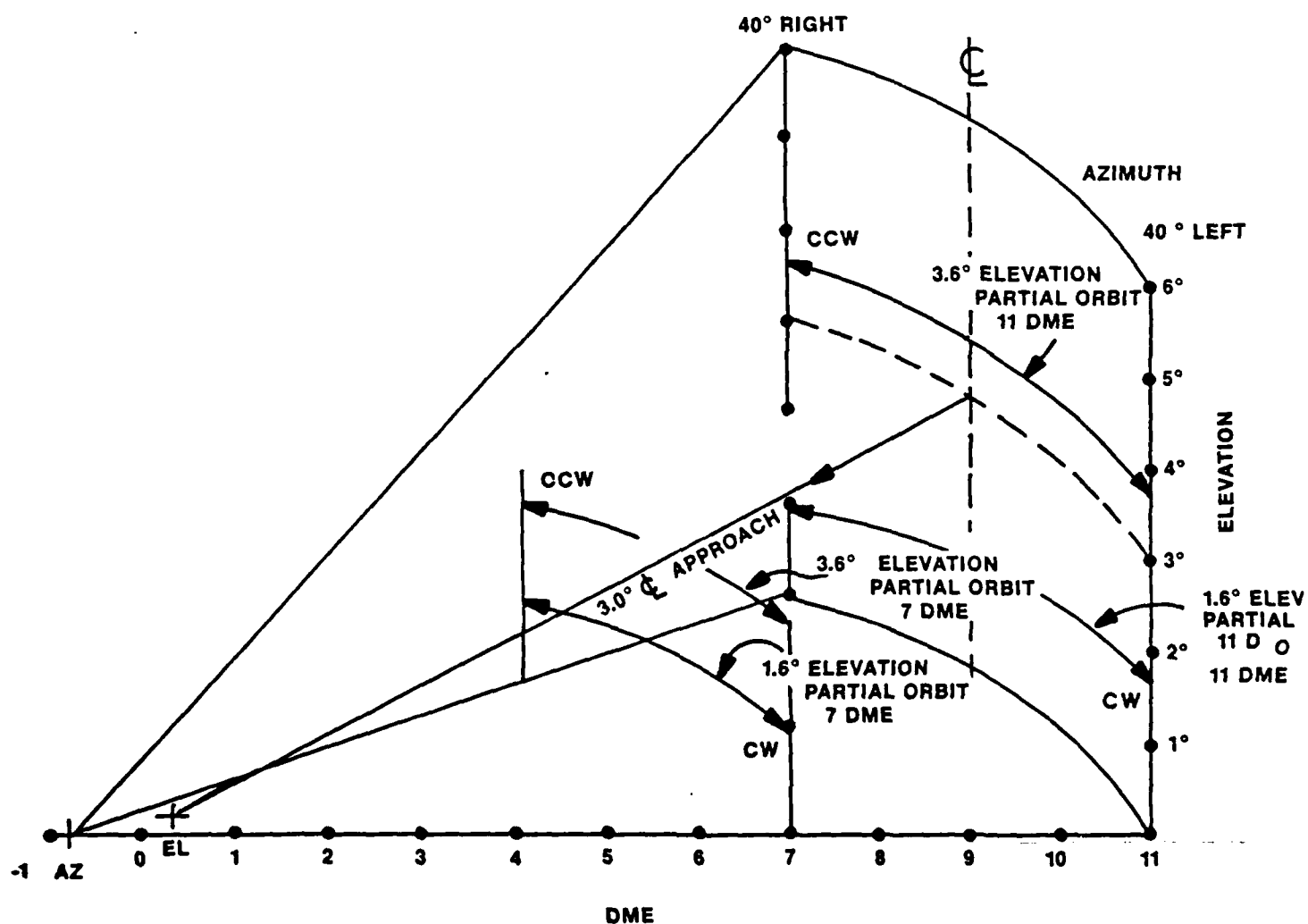
FIGURE 2.   ENGINEERING FLIGHT TEST PROFILES

MLS AIRBORNE DATA PROCESSED BY:
FAA TECHNICAL CENTER, ACD-330
ATLANTIC CITY AIRPORT, NJ 08405

TITLE: CW ORBIT 7 DME 3000 FT. 3.6 O/S
RUNWAY: 22L   AIRPORT: CHICAGO MIDWAY
TAPE ID: MDW0827   RUN #:06   DATE:08/27/88   START: 06:39:44.008   STOP: 06:43:00.817
AZIMUTH SYSTEM ONE
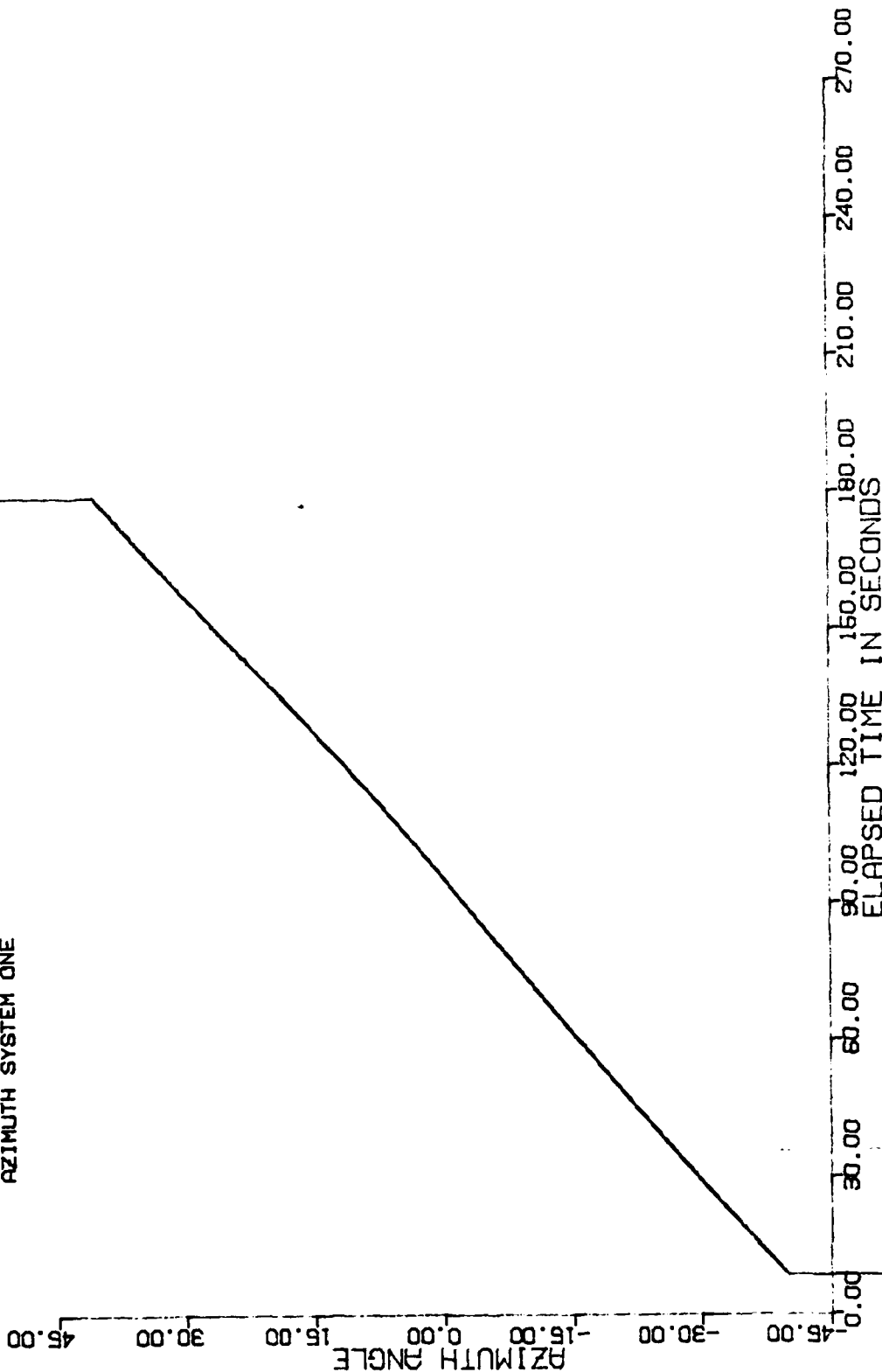
FIGURE 3. CLOCKWISE ORBIT AT 3.6 DEGREE ELEVATION ANGLE, 7 DME FROM DME.
AZIMUTH SYSTEM 1. AIRBORNE ANGLE DATA

11

MLS AIRBORNE DATA PROCESSED BY:
            FAA TECHNICAL CENTER, ACD-330
            ATLANTIC CITY AIRPORT, NJ 08405

TITLE: CW ORBIT 11 DME 2400 FT. 1.6 D/S
RUNWAY: 22L   AIRPORT: CHICAGO MIDWAY
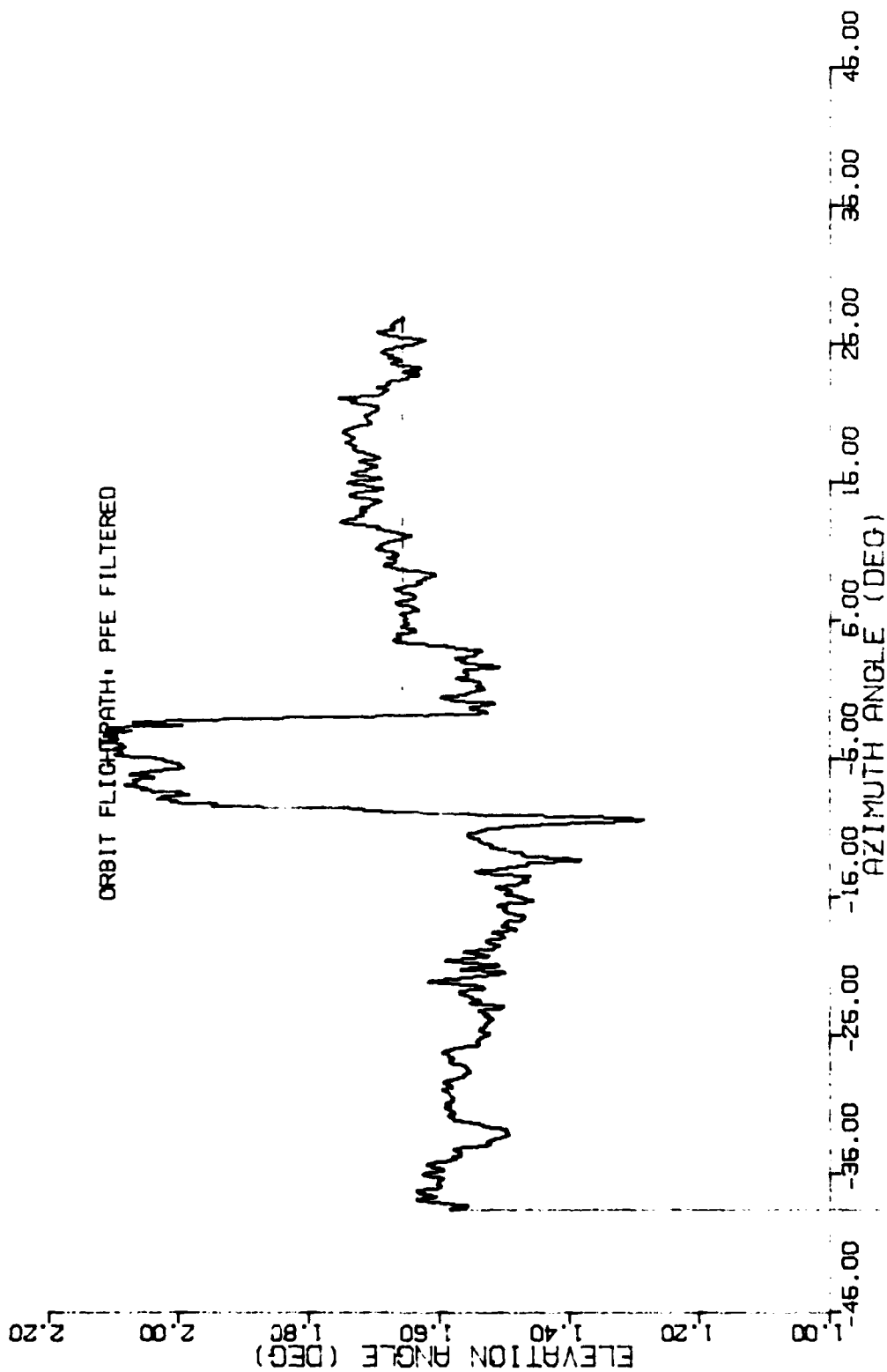TAPE ID: MDW0827   RUN #:04   DATE:08/27/88   START: 06:26:23.009   STOP: 06:31:15.847
AZIMUTH SYSTEM ONE
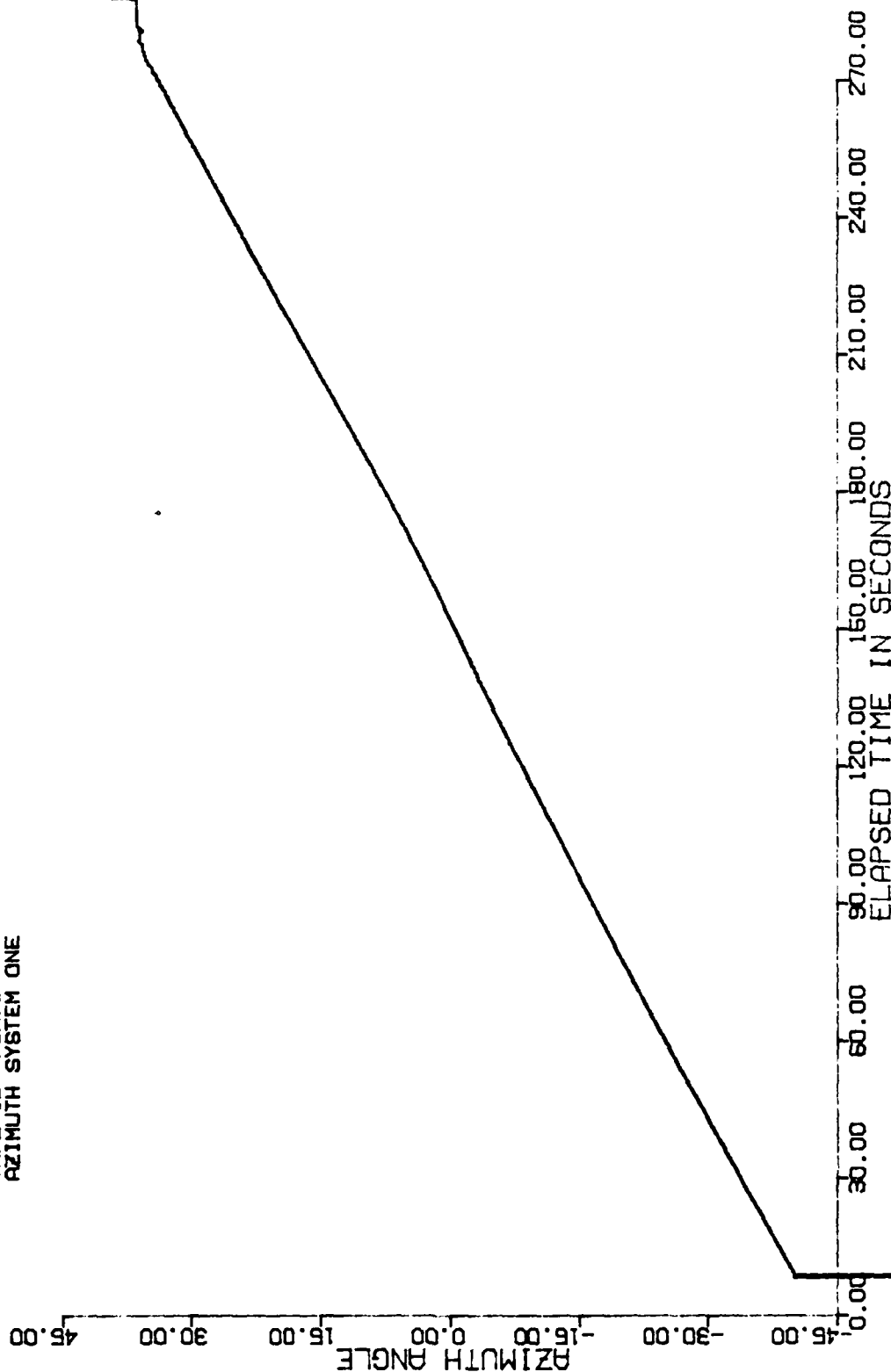
FIGURE 4.   CLOCKWISE ORBIT AT 1.6 DEGREE ELEVATION ANGLE. 11 NMI FROM DME.
            AZIMUTH SYSTEM 1. AIRBORNE ANGLE DATA

12

ML6 MATHEMATICAL MODELING PERFORMED BY:
FAA TECHNICAL CENTER, GUIDANCE BRANCH
ATLANTIC CITY AIRPORT, NJ 08405

TITLE: MDW0827, CCW ORBIT, 11 DME, 4900 FT., 3.6 G/S
RUN #: 0001 DATE : 8-DEC-89   12:55:56
RUNWAY, 22L   AIRPORT,MIDWAY AIRPORT, CHICAGO, ILLINOIS
ANTENNA, AZBL2040 BEAMWIDTH=2.00

AZ DYNAMIC SPLIT

AZIMUTH ANGLE (DEG)

ERROR (DEG)

12-DEC-89 14:12:28
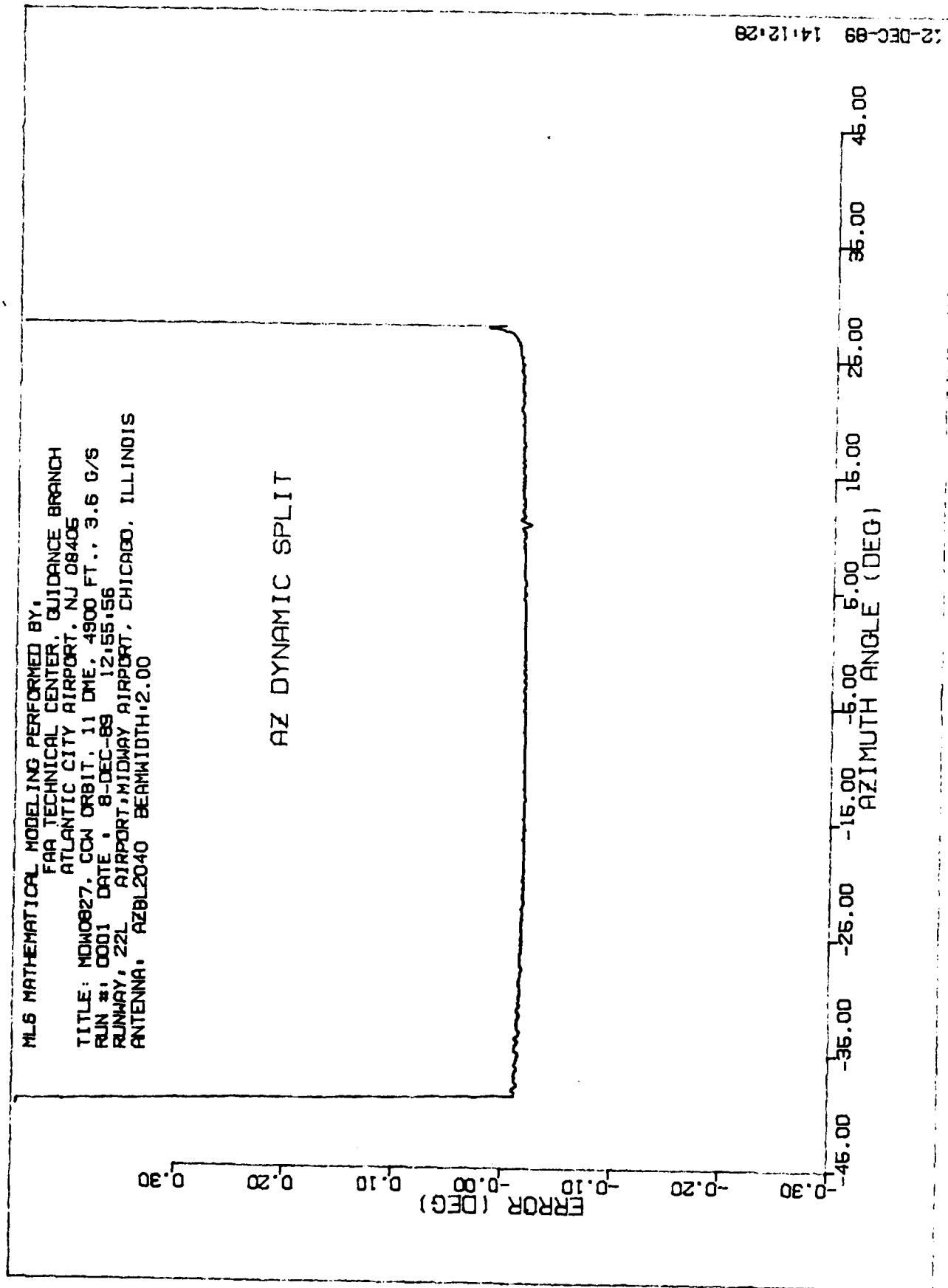
FIGURE 5.   COUNTERCLOCKWISE ORBIT AT 3.6 DEGREE ELEVATION ANGLE, 11 NMI FROM DME. AZIMUTH SYSTEM. MODEL DYNAMIC ERROR PLOT

13
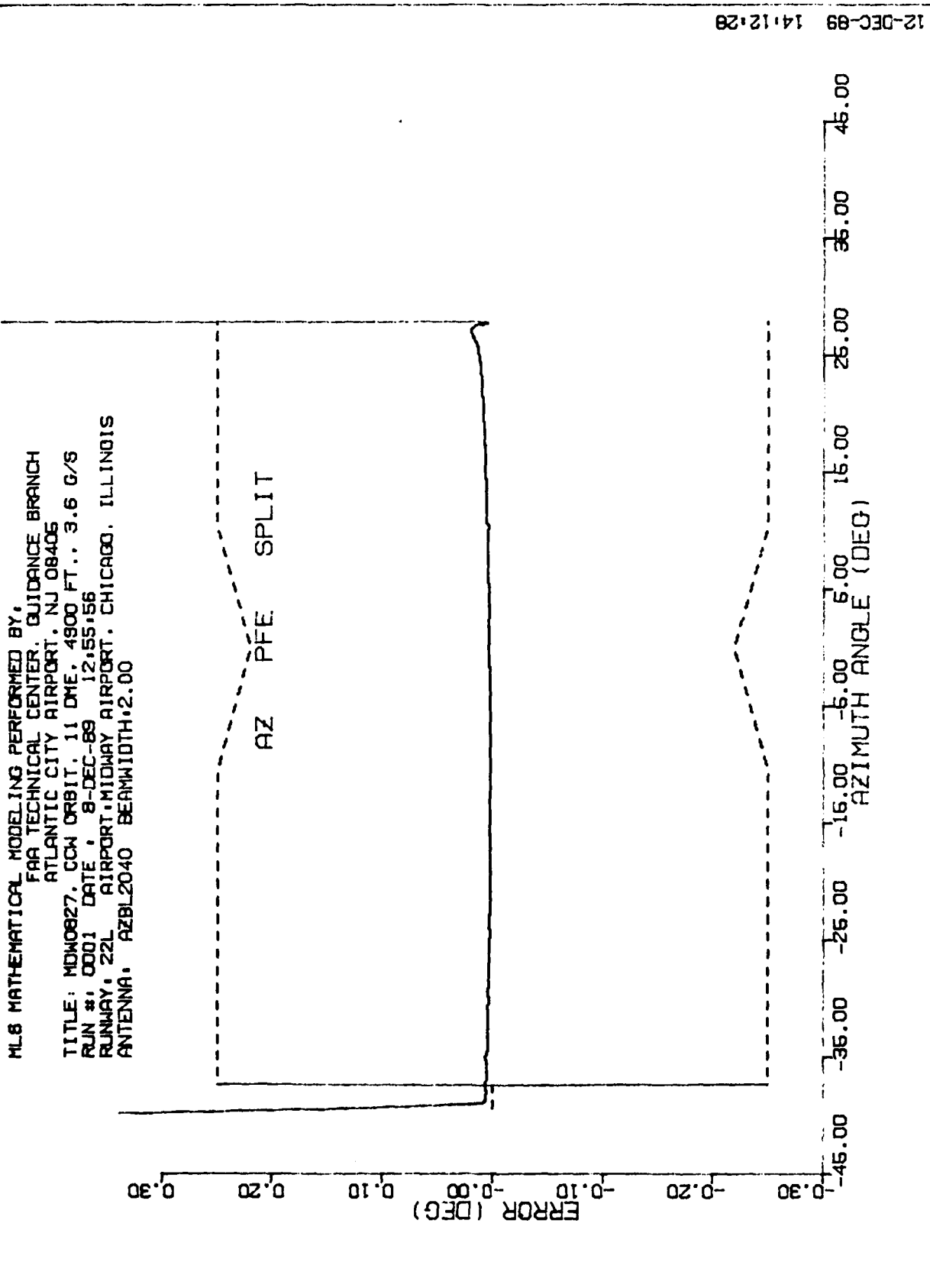
FIGURE 6. COUNTERCLOCKWISE ORBIT AT 3.6 DEGREE ELEVATION ANGLE, 11 NMI FROM
DME, AZIMUTH SYSTEM. MODEL PFE FILTERED ERROR PLOT

14
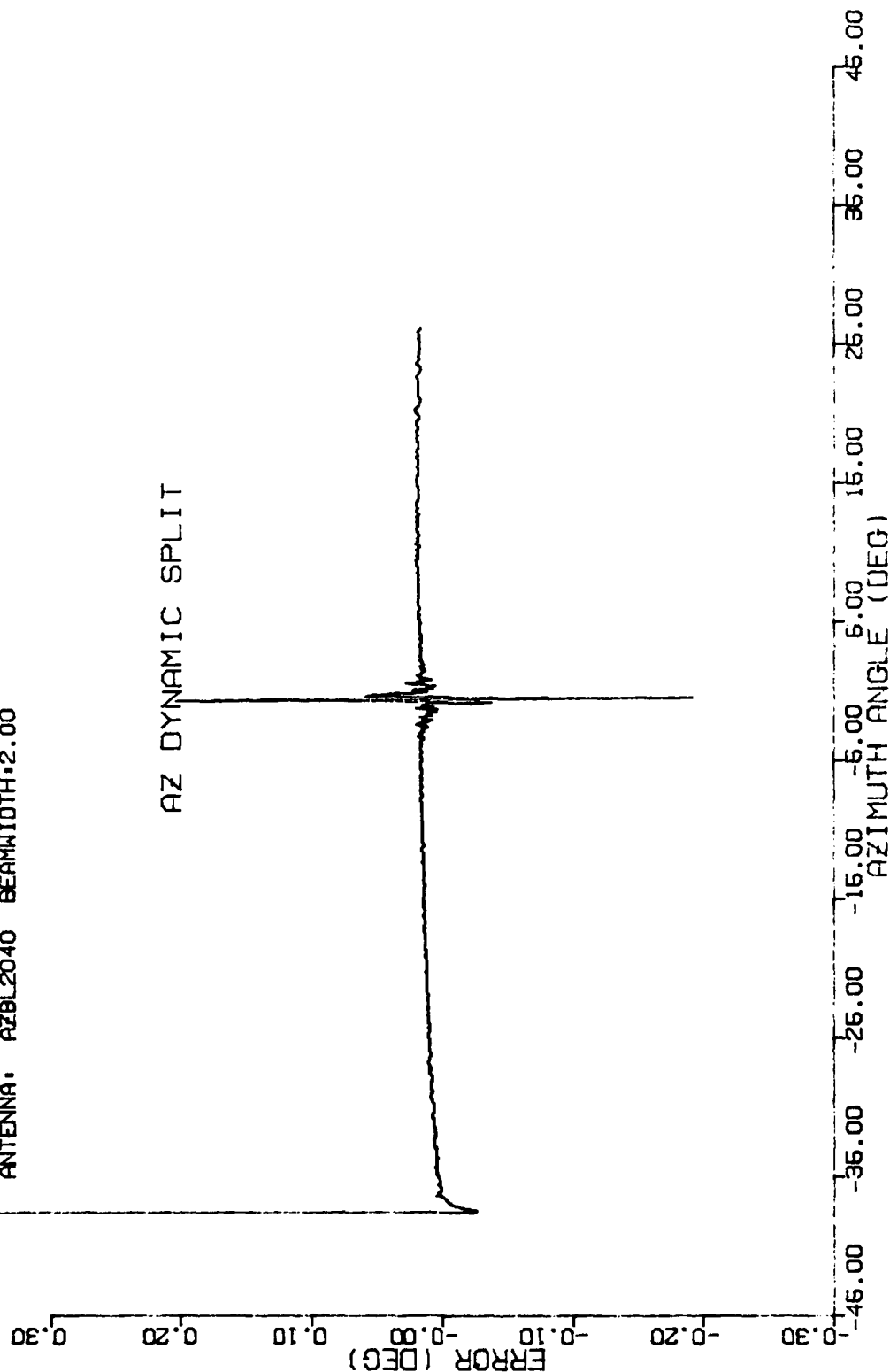
FIGURE 7. CLOCKWISE ORBIT AT 1.6 DEGREE ELEVATION ANGLE, 11 NMI FROM DME, AZIMUTH SYSTEM, MODEL DYNAMIC ERROR PLOT.

FIGURE 8. CLOCKWISE ORBIT AT 1.6 DEGREE ELEVATION ANGLE, 11 NMI FROM DME, AZIMUTH SYSTEM, MODEL PFE FILTERED ERROR PLOT

A.
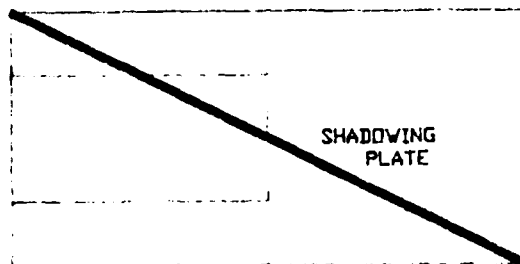
SHADOWING
PLATE

TO MIDWAY AIRPORT

B.
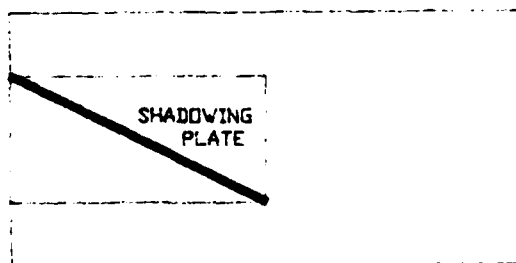
SHADOWING
PLATE

TO MIDWAY AIRPORT

FIGURE 9.   TOP VIEW OF SHADOWING PLATES FOR SEARS TOWER

17

FIGURE 10. CLOCKWISE ORBIT AT 1.6 DEGREE ELEVATION ANGLE, 11 NMI FROM DME, AZIMUTH SYSTEM, MODEL DYNAMIC ERROR PLOT
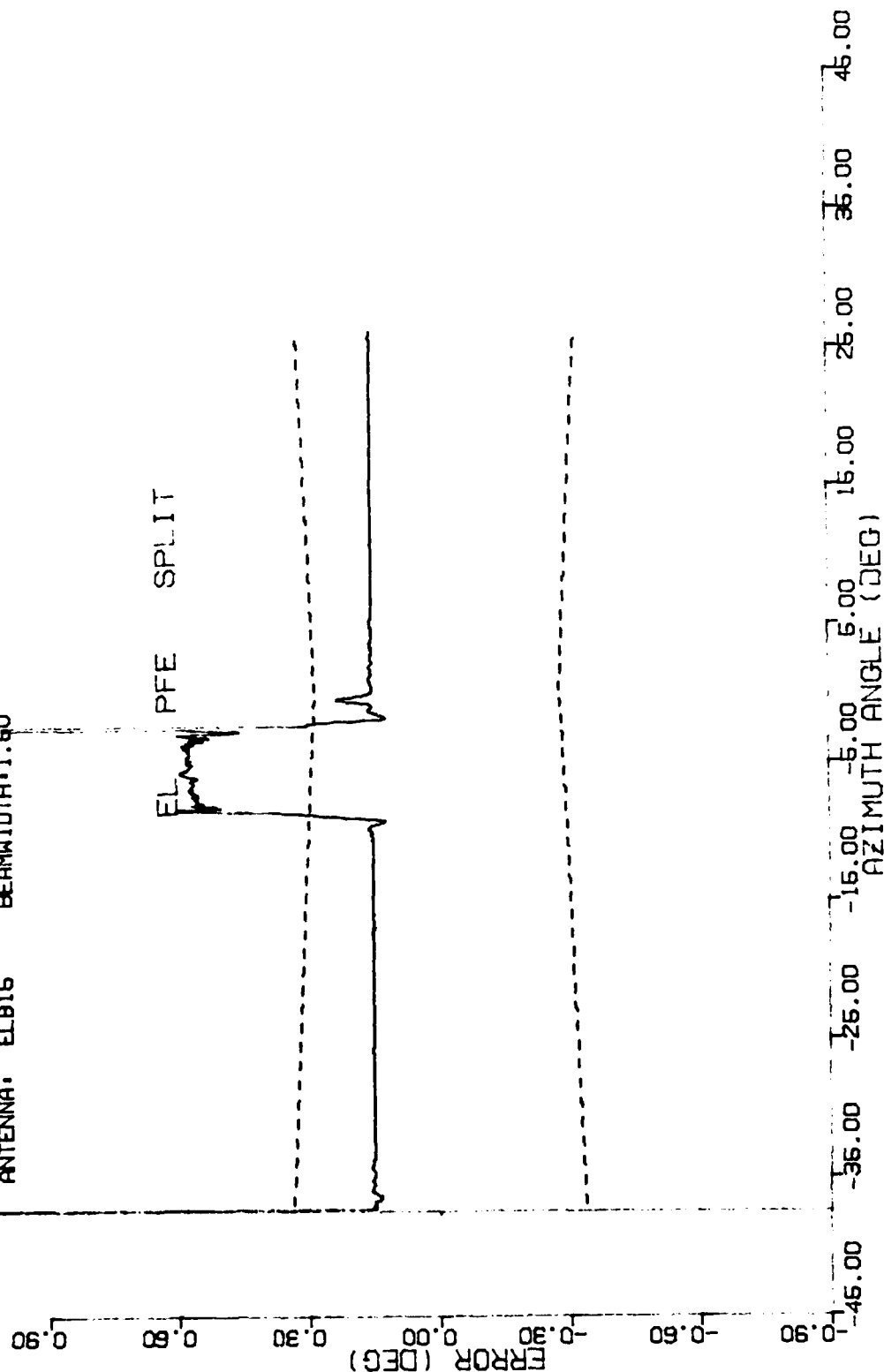
FIGURE 11. CLOCKWISE ORBIT AT 1.6 DEGREE ELEVATION ANGLE, 11 NMI FROM DME.
ELEVATION SYSTEM, MODEL PFE FILTERED ERROR PLOT

MLS AIRBORNE DATA PROCESSED BY:
FAA TECHNICAL CENTER, ACD-330
ATLANTIC CITY AIRPORT, NJ 08405

TITLE: CW ORBIT 11 DME 2400 FT, 1.6 0/S
RUNWAY: 22L   AIRPORT: CHICAGO MIDWAY
TAPE ID: MDW0827   RUN #:04   DATE:08/27/88

ORBIT FLIGHTPATH: PFE FILTERED

FIGURE 12.   CLOCKWISE ORBIT AT 1.6 DEGREE ELEVATION ANGLE, 11 DME FROM DME.
ELEVATION SYSTEM, AIRBORNE ANGLE DATA

20
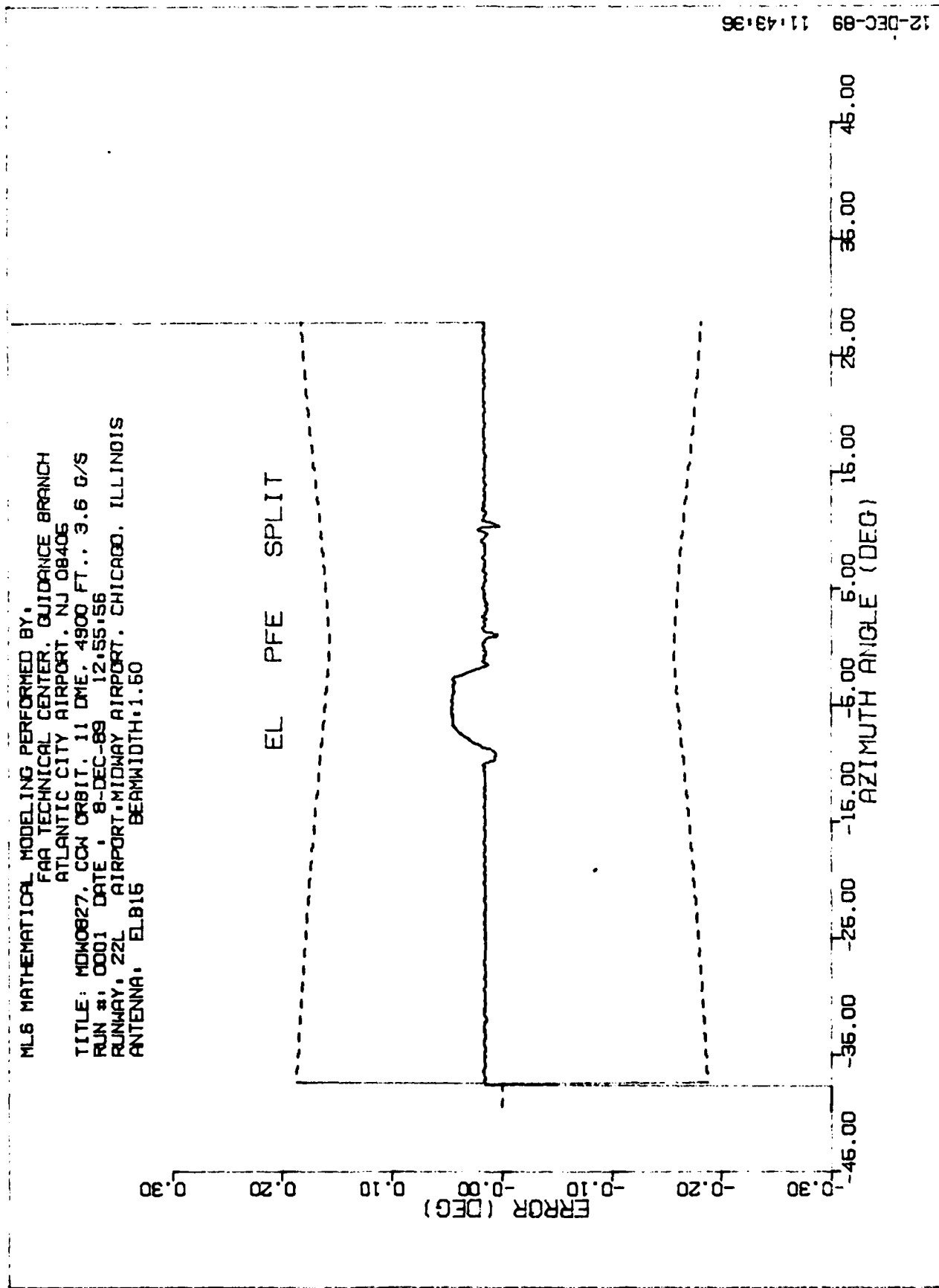
FIGURE 13. COUNTERCLOCKWISE ORBIT AT 3.6 DEGREE ELEVATION ANGLE, 11 NMI FROM DME, ELEVATION SYSTEM. MODEL PFE FILTERED ERROR PLOT

FIGURE 14. COUNTERCLOCKWISE ORBIT AT 3.6 DEGREE ELEVATION ANGLE, 11 NMI FROM DME. ELEVATION SYSTEM. AIRBORNE ANGLE DATA
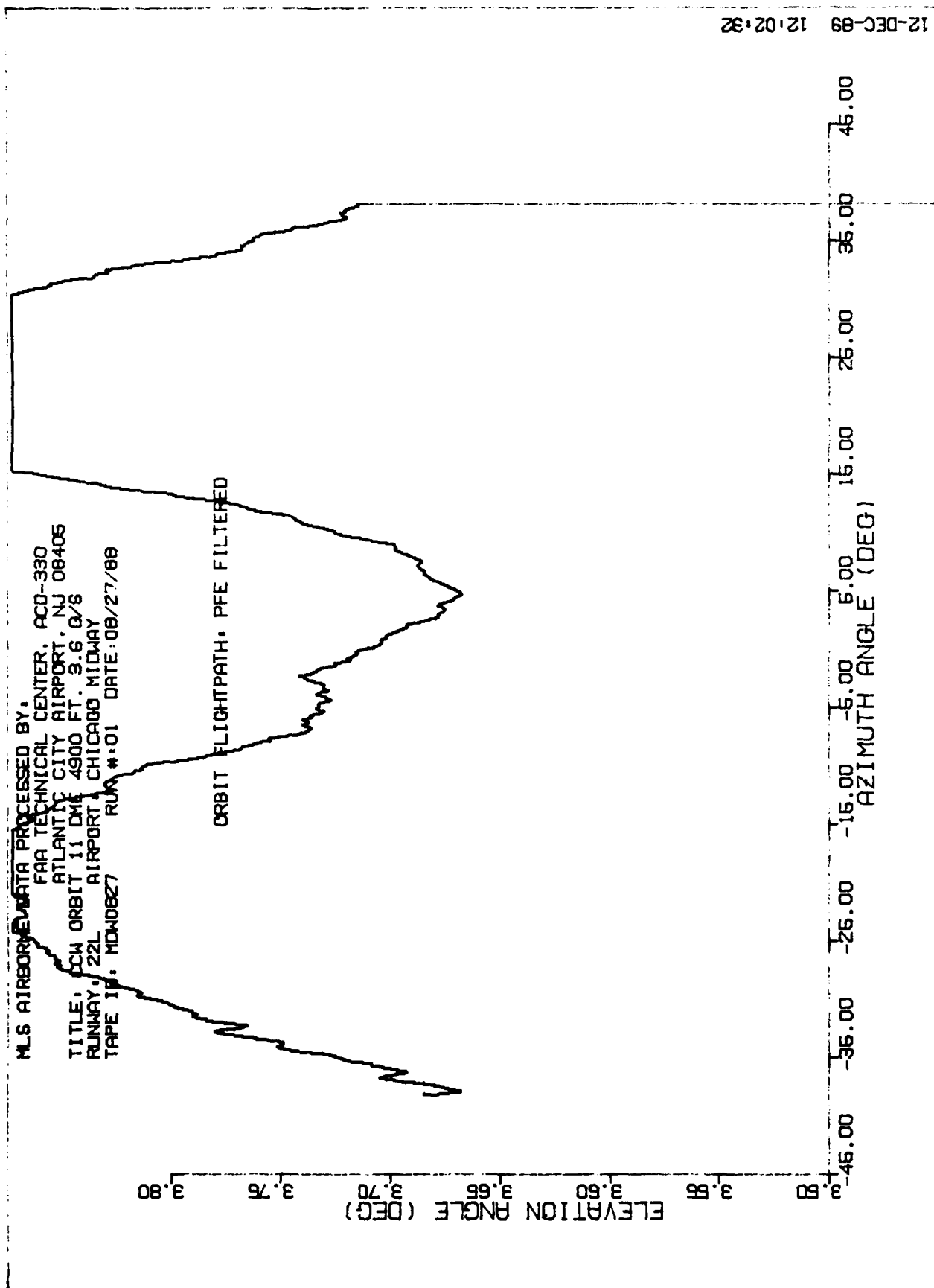
FIGURE 15. COUNTERCLOCKWISE ORBIT AT 3.6 DEGREE ELEVATION ANGLE, 11 NM1
            FROM DME, ELEVATION SYSTEM, AIRBORNE ANGLE DATA

MLS AIRBORNE DATA PROCESSED BY:
        FAA TECHNICAL CENTER, ACD-330
        ATLANTIC CITY AIRPORT, NJ 08405

TITLE: 3.6 DEGREE APPROACH
RUNWAY: 22L   AIRPORT, CHICAGO MIDWAY
TAPE ID: MDW08Z7   RUN #:07   DATE:08/27/88
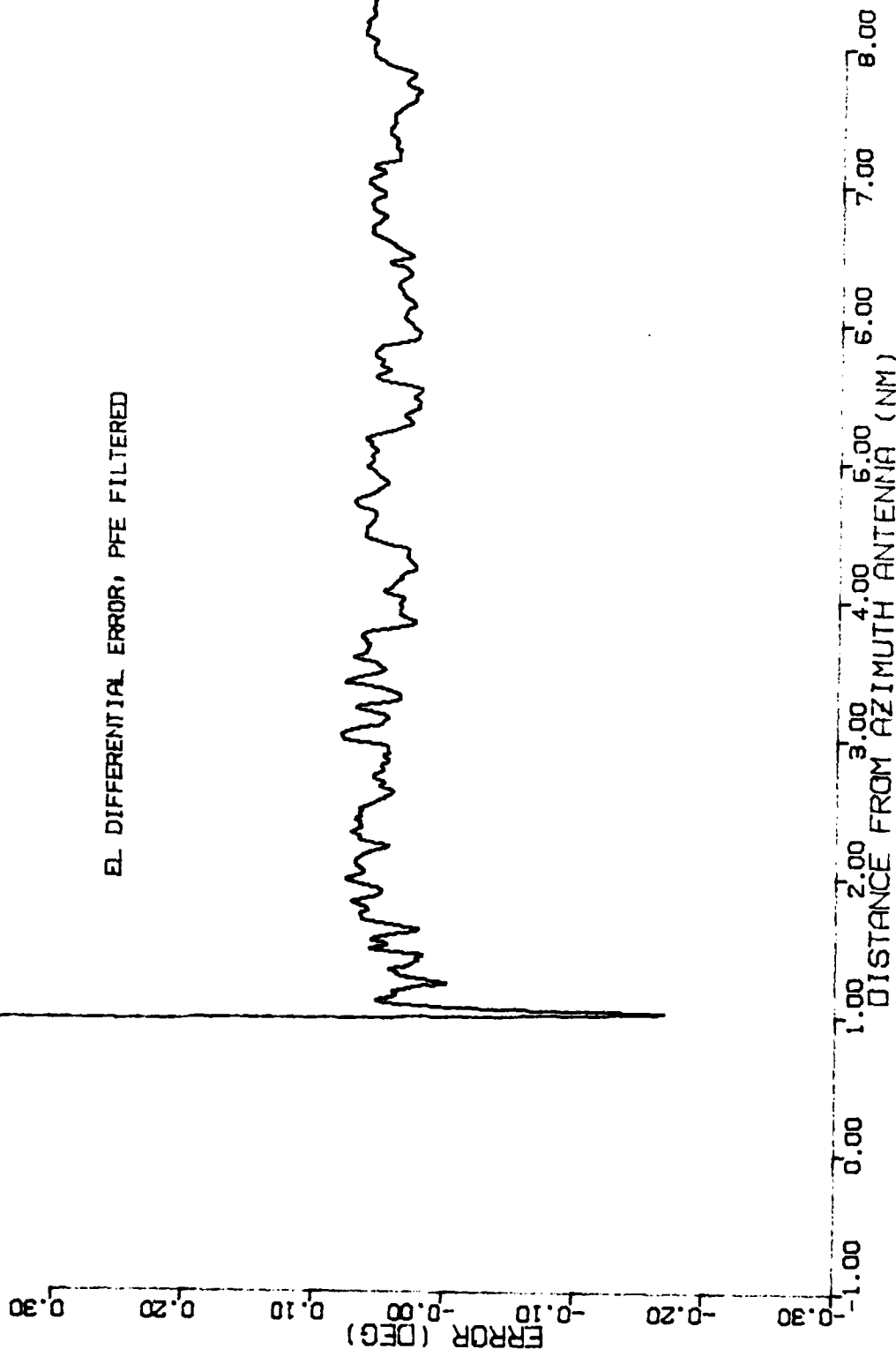
AZ DIFFERENTIAL ERROR, PFE FILTERED

FIGURE 16.   CENTERLINE APPROACH AT 3.6 DEGREE ELEVATION ANGLE. AZIMUTH
             SYSTEM, AIRBORNE DIFFERENTIAL ERROR PLOT

24
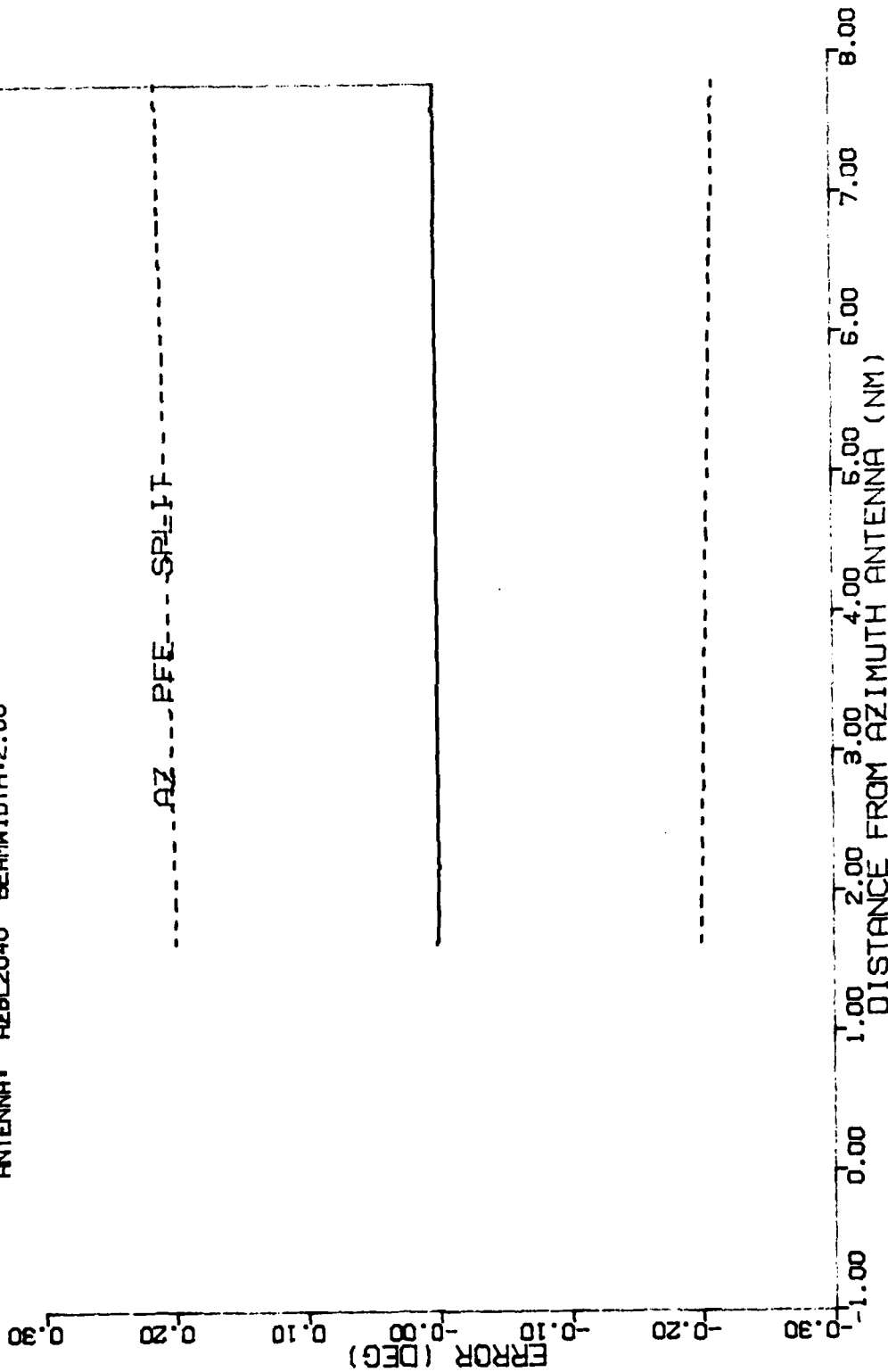
FIGURE 17. CENTERLINE APPROACH AT 3.6 DEGREE ELEVATION ANGLE, AZIMUTH SYSTEM, MODEL PFE FILTERED ERROR PLOT

FIGURE 18.   CENTERLINE APPROACH AT 3.4 DEGREE ELEVATION ANGLE, ELEVATION
SYSTEM, AIRBORNE DIFFERENTIAL ERROR PLOT
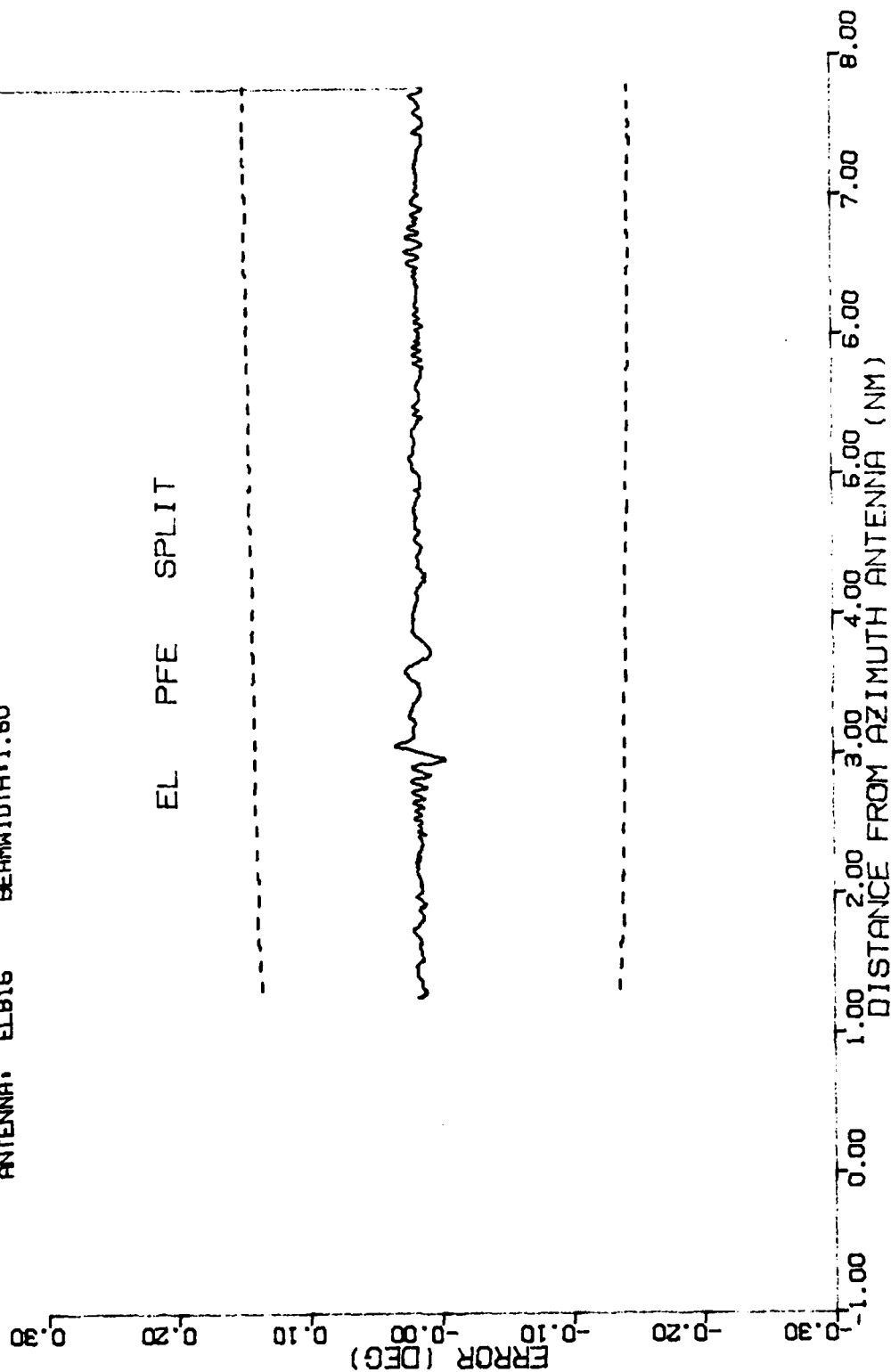
FIGURE 19. CENTERLINE APPROACH AT 3.4 DEGREE ELEVATION ANGLE. ELEVATION SYSTEM. MODEL PFE FILTERED ERROR PLOT

27

MLS AIRBORNE DATA PROCESSED BY,
FAA TECHNICAL CENTER, ACD-330
ATLANTIC CITY AIRPORT, NJ 08405

TITLE: 3.0 DEGREE APPROACH
RUNWAY: 22L   AIRPORT, CHICAGO MIDWAY
TAPE ID, MDW0829   RUN #:06   DATE:08/29/88

EL DIFFERENTIAL ERROR, PFE FILTERED

ERROR (DEG)

DISTANCE FROM AZIMUTH ANTENNA (NM)

FIGURE 20.   CENTERLINE APPROACH AT 3.0 DEGREE ELEVATION ANGLE, ELEVATION
SYSTEM, AIRBORNE DIFFERENTIAL ERROR PLOT

28

MLS MATHEMATICAL MODELING PERFORMED BY:
FAA TECHNICAL CENTER, GUIDANCE BRANCH
ATLANTIC CITY AIRPORT, NJ 08405

TITLE: MDW0829, 3.0 DEGREE APPROACH
RUN #: 0006   DATE : 22-JUN-89   09:13:49
RUNWAY: 22L   AIRPORT:MIDWAY AIRPORT, CHICAGO, ILLINOIS
ANTENNA: ELB16   BEAMWIDTH:1.60

EL   PFE   SPLIT

DISTANCE FROM AZIMUTH ANTENNA (NM)

ERROR (DEG)
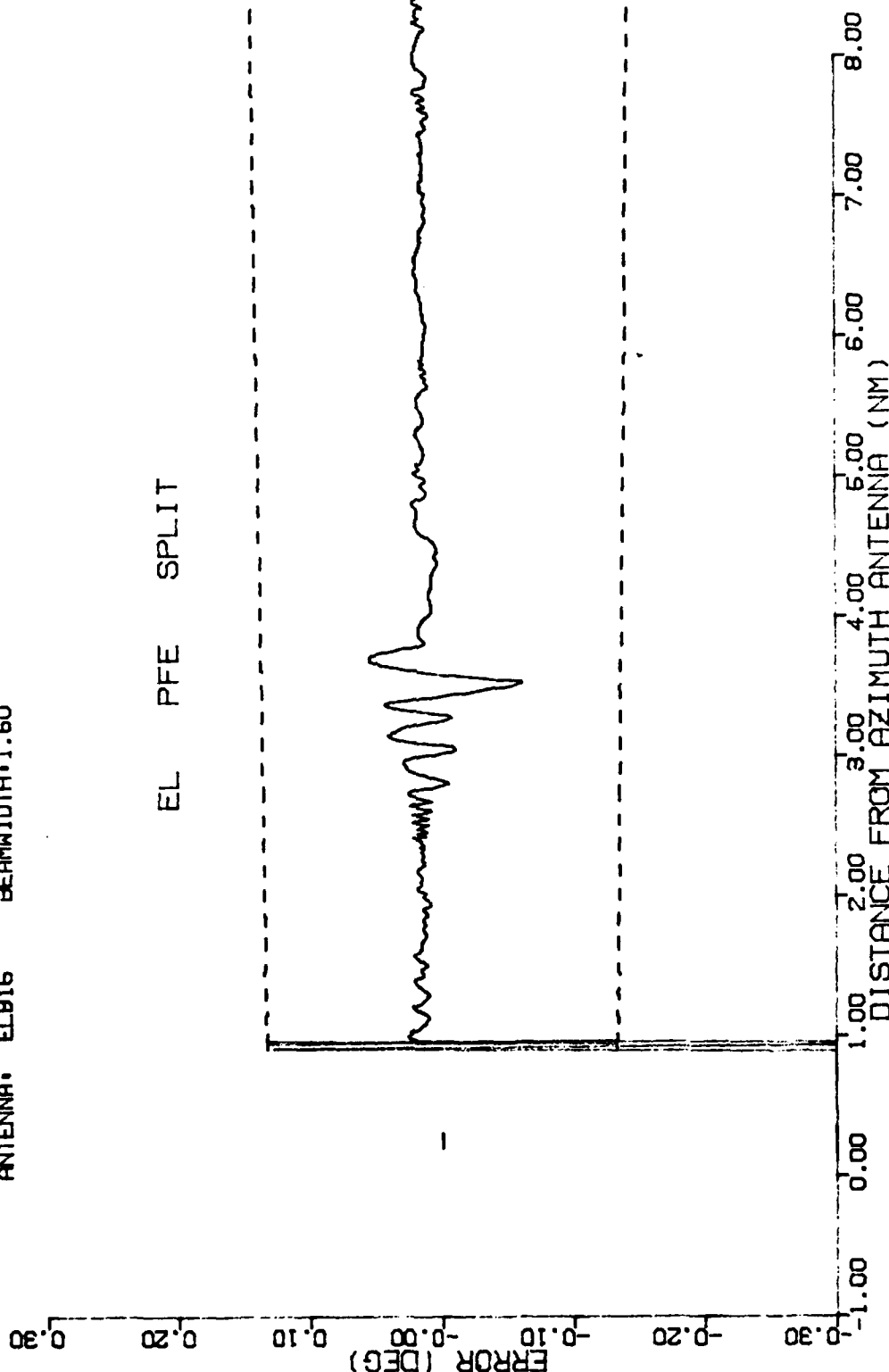
11-DEC-89   13:24:29

FIGURE 21.   CENTERLINE APPROACH AT 3.0 DEGREE ELEVATION ANGLE, ELEVATION
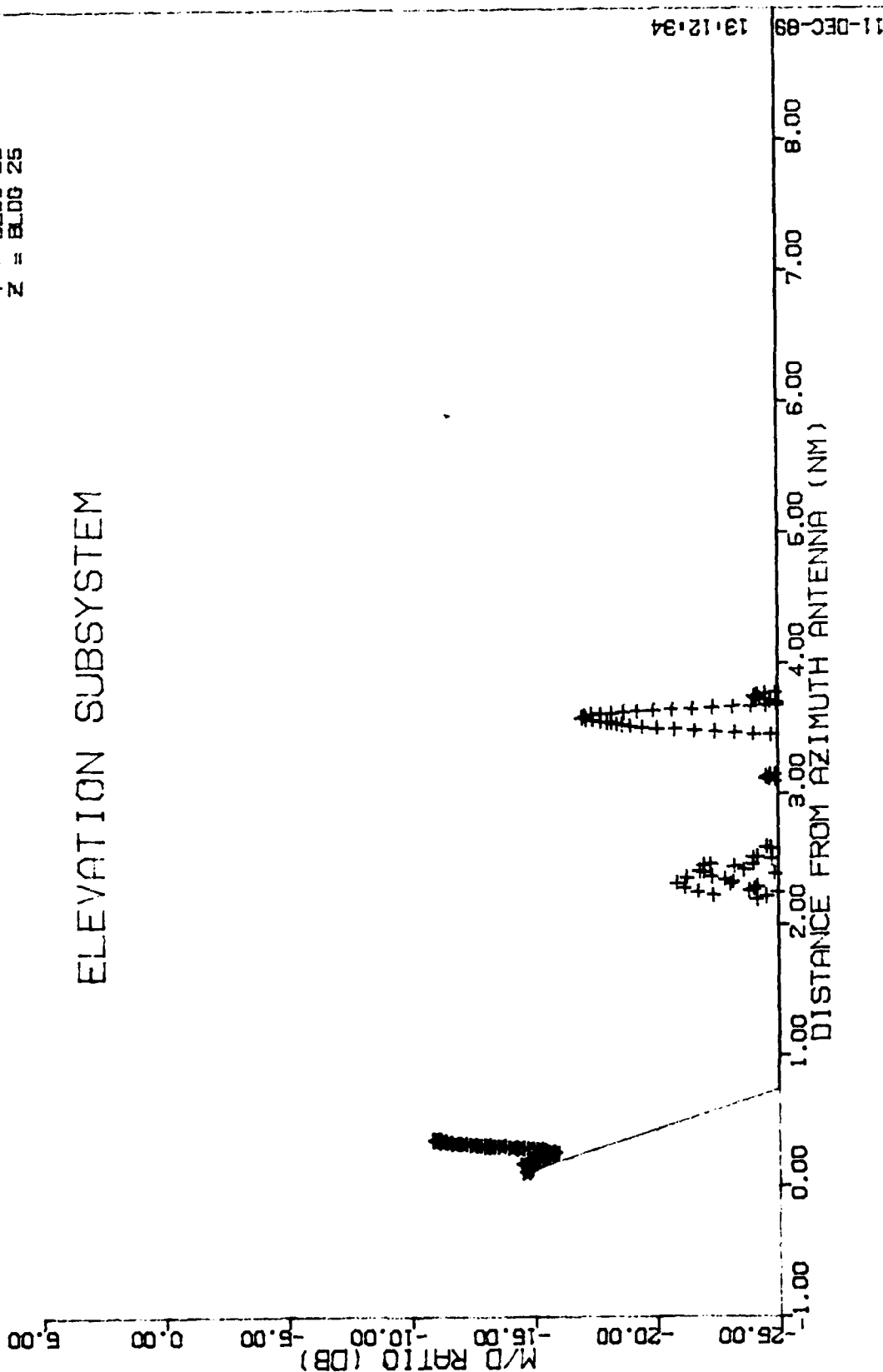SYSTEM, MODEL PFE FILTERED ERROR PLOT

29

FIGURE 22. CENTERLINE APPROACH AT 3.0 DEGREE ELEVATION ANGLE, ELEVATION
SYSTEM. MODEL MULTIPATH/DIRECT RATIO PLOT

MLS MATHEMATICAL MODELING PERFORMED BY,
FAA TECHNICAL CENTER, GUIDANCE BRANCH
ATLANTIC CITY AIRPORT, NJ 08406

TITLE: MDW0829, 3.0 DEGREE APPROACH
RUN #: 0006   DATE, 7-DEC-89   11:42:50
RUNWAY, 22L   AIRPORT:MIDWAY AIRPORT, CHICAGO, ILLINOIS

PLOT SYMBOLS
* = BLDG 4
+ = BLDG 9
O = BLDG 6
X = GROUND
Y = BLDG 10
Z = BLDG 21

ELEVATION SUBSYSTEM

DISTANCE FROM AZIMUTH ANTENNA (KM)

M/D RATIO (DB)

FIGURE 23.   CENTERLINE APPROACH AT 3.0 DEGREE ELEVATION ANGLE, ELEVATION
SYSTEM, MODEL MULTIPATH/DIRECT RATIO PLOT, ROUGHNESS = 0.2

31

MLS MATHEMATICAL MODELING PERFORMED BY:
FAA TECHNICAL CENTER, GUIDANCE BRANCH
ATLANTIC CITY AIRPORT, NJ 08405

TITLE: MDW0829, 3.0 DEGREE APPROACH
RUN #: 0006 DATE : 7-DEC-89   12:10:48
RUNWAY: 22L   AIRPORT:MIDWAY AIRPORT, CHICAGO, ILLINOIS
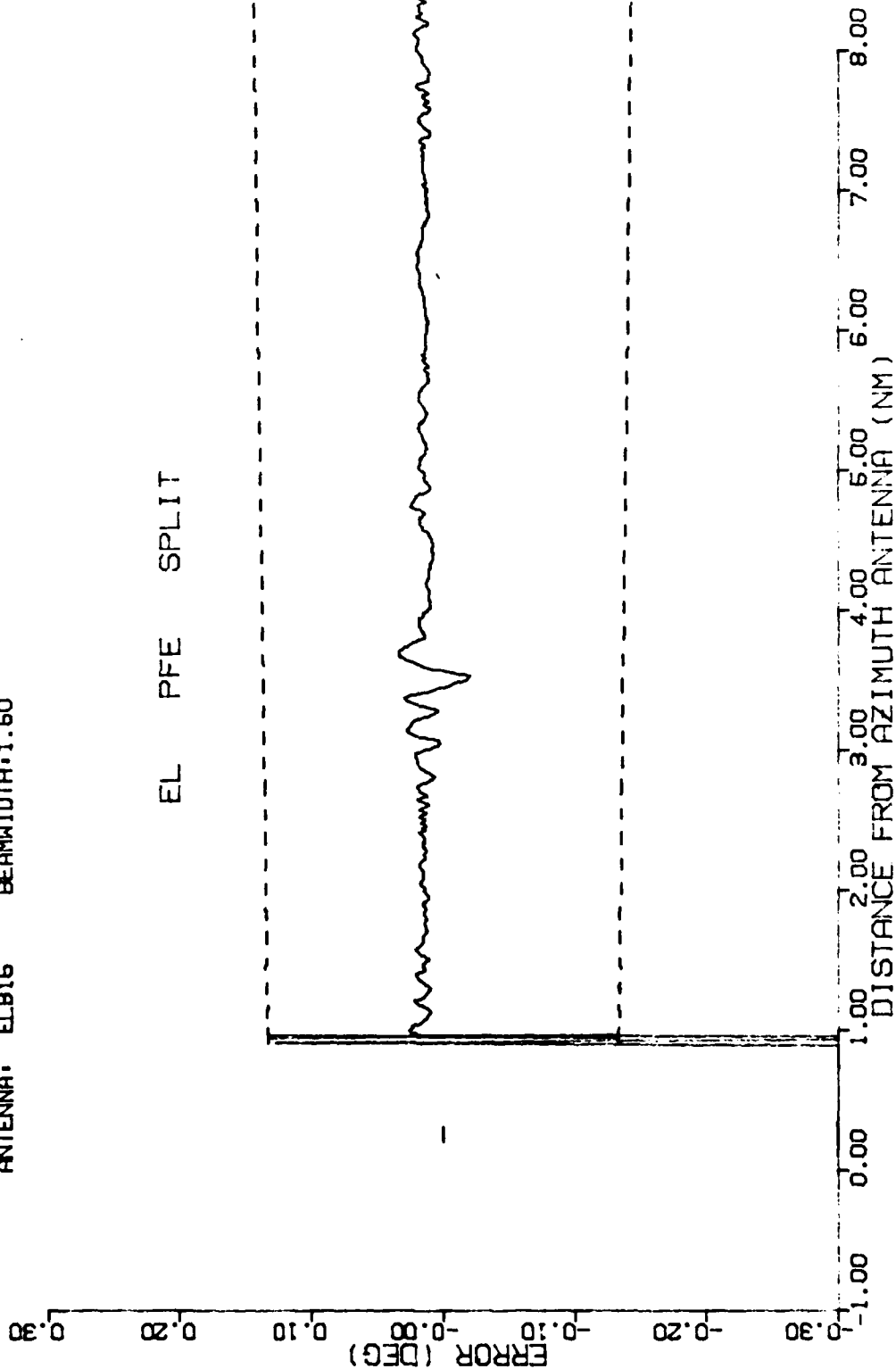ANTENNA: ELB16   BEAMWIDTH:1.50

EL PFE SPLIT

11-DEC-89 10:00:18

FIGURE 24. CENTERLINE APPROACH AT 3.0 DEGREE ELEVATION ANGLE, ELEVATION
SYSTEM, MODEL PFE FILTERED ERROR PLOT, ROUGHNESS = 0.2

DISTANCE FROM AZIMUTH ANTENNA (NM)

ERROR (DEG)

09:36:46   11-DEC-89

PLOT SYMBOLS

```
# = BLDG 9
+ = BLDG 4
0 = GROUND
X = BLDG 6
Y = BLDG 10
Z = BLDG 21
```

ML8 MATHEMATICAL MODELING PERFORMED BY,
FAA TECHNICAL CENTER, GUIDANCE BRANCH
ATLANTIC CITY AIRPORT, NJ 08405

TITLE: MDW0829, 3.0 DEGREE APPROACH
RUN #: 0006   DATE, 7-DEC-89   15:37:54
RUNWAY, 22L   AIRPORT,MIDWAY AIRPORT, CHICAGO, ILLINOIS

ELEVATION SUBSYSTEM

DISTANCE FROM AZIMUTH ANTENNA (NM)

M/D RATIO (DB)

FIGURE 25.   CENTERLINE APPROACH AT 3.0 DEGREE ELEVATION ANGLE, ELEVATION
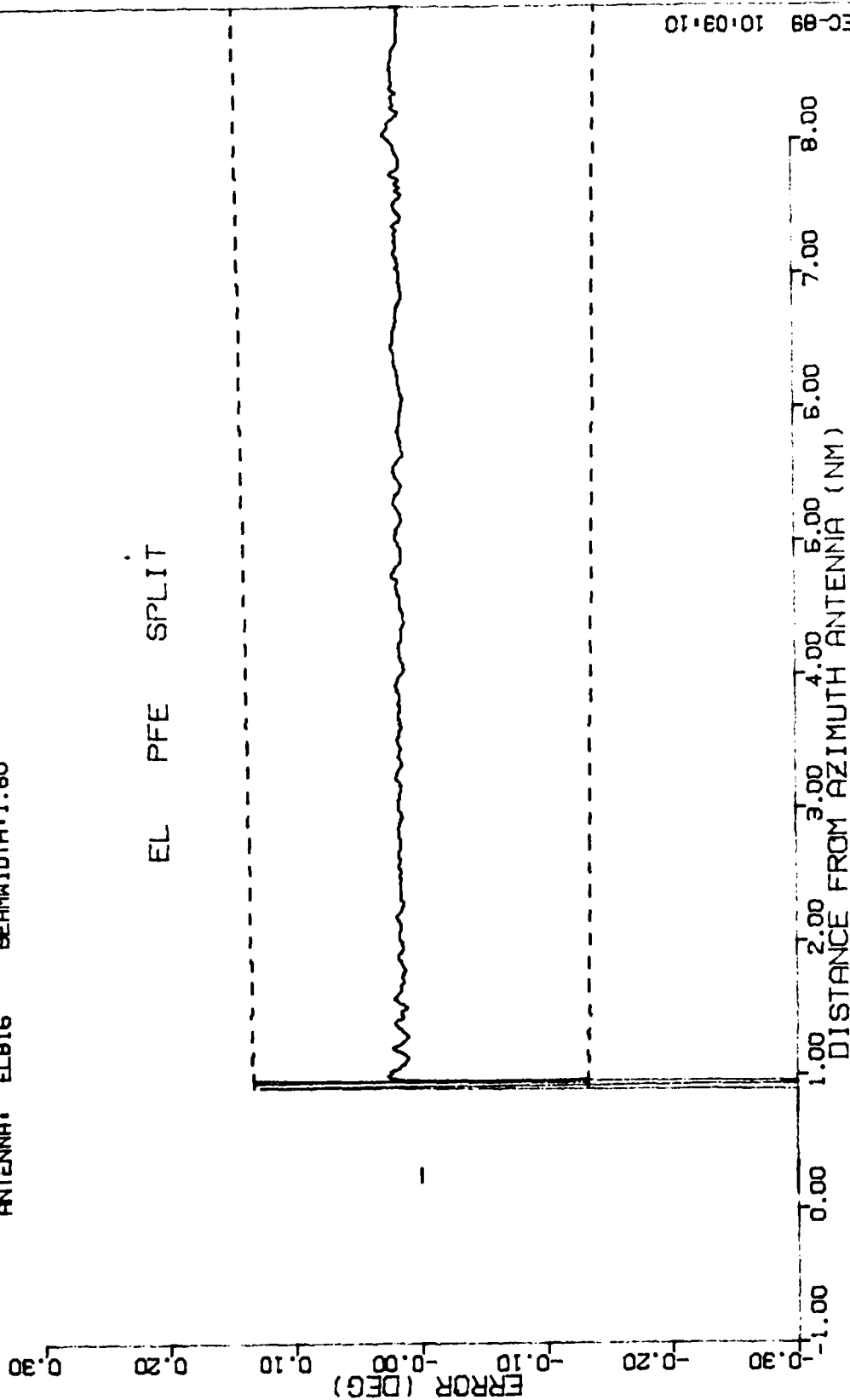SYSTEM, MODEL MULTIPATH/DIRECT RATIO PLOT, ROUGHNESS = 0.5

33

FIGURE 26. CENTERLINE APPROACH AT 3.0 DEGREE ELEVATION ANGLE. ELEVATION
SYSTEM. MODEL PFE FILTERED ERROR PLOT. ROUGHNESS = 0.5